Bacterial Diversity in Clay and Actinide Interactions with Bacterial Isolates in Relation to Nuclear Waste Disposal

Henry Moll, Laura Lütke, and Andrea Cherkouk

Contents

Abstract One potential source of actinides (An) in the environment could be the accidental release from nuclear waste disposal sites. Hence, the long-term safety of nuclear waste in a deep geologic repository is an important issue in our society. Microorganisms indigenous to potential host rocks are able to influence the speciation and therefore the mobility of An and their retardation both by direct and indirect pathways. They can as well affect the conditions in a geologic repository (e.g., by gas generation or canister corrosion). The focus of this chapter lies on the influence of indigenous microbes on the speciation of An. Therefore, for the safety assessment of such a repository, it is necessary to know which microorganisms are present in the potential host rocks (clay and salt) and if these microorganisms can influence the speciation of released An. Hence, dominant bacterial strains from potential host rocks for future nuclear waste depositions have to be investigated regarding their interaction mechanisms with soluble An ions. This chapter will cover the following research areas. Gained knowledge concerning the bacterial diversity in, e.g., Mont Terri Opalinus clay by applying direct molecular culture-

H. Moll (✉) • A. Cherkouk
Helmholtz-Zentrum Dresden-Rossendorf, Institute of Resource Ecology, Bautzner Landstraße 400, 01328 Dresden, Germany
e-mail: h.moll@hzdr.de

L. Lütke
Institut für Radioökologie und Strahlenschutz (IRS), Leibniz Universität Hannover, 30419 Hannover, Germany

C. Walther, D.K. Gupta (eds.), *Radionuclides in the Environment*,
DOI 10.1007/978-3-319-22171-7_12

independent retrievals and cultivation experiments will be presented. Their influence on the geochemical behavior of selected An (uranium and curium) will be highlighted. These investigations contribute to a better understanding of microbial interactions of An on a molecular level for an improved prediction of the safety of a planned nuclear waste repository.

Keywords Bacterial diversity • Bacteria • Complexation • Uranium • Curium • *Sporomusa* sp. • *Paenibacillus* sp. • TRLFS • Potentiometry

1 Introduction

Besides the prominent processes influencing the migration of An in the environment, e.g., sorption onto mineral surfaces, there is growing attention to the influence of indigenous microorganisms on their speciation. The comprehensive concept of geological disposal comprises a detailed knowledge concerning potential host rock formations. One of such formations is the Opalinus clay formations of the Mont Terri underground rock laboratory (URL), Switzerland, which is under investigation to test their suitability as host rock for future disposal of radioactive waste (Thury and Bossart 1999). Enriched bacteria indigenous to such subterranean soil environments can affect the speciation and hence the mobility of released An (Lovley et al. 1991; Kalinowski et al. 2004; Merroun and Selenska-Pobell 2008; Lloyd and Gadd 2011; Anderson et al. 2011; Brookshaw et al. 2012; Lütke et al. 2013; Moll et al. 2014). Therefore, it is of importance to identify relevant interaction processes occurring with dominant bacterial strains isolated from mentioned sites destined for the safe disposal of nuclear waste and to assess the resulting actinide speciation. Bacteria belong to the most widely spread organisms in nature. Besides archaea, these organisms represent the only form of life which can inhabit hostile environments of, e.g., high salinity (Oren 2002), temperature (Takai et al. 2008), and radiation (Makarova et al. 2001), like in designated nuclear waste disposal sites.

In general, the versatile interactions between microbes and An can be classified into two major categories: the direct and indirect interaction mechanisms. Direct interactions include the processes bioaccumulation, biosorption, biomineralization, and biotransformation (Fig. 1). Bioaccumulation means the incorporation of the An inside the cell (Brockmann et al. 2014; Günther et al. 2014; Merroun and Selenska-Pobell 2008; Suzuki and Banfield 2004). Biosorption describes a pure binding of the An to surface functional groups of the respective cell envelope (Reitz et al. 2014; Günther et al. 2014; Moll et al. 2014; Lütke et al. 2012, 2013; Markai et al. 2003; Texier et al. 2000; Fowle et al. 2000). Biomineralization refers to the cellular liberation of inorganic ligands leading to the formation of a precipitate, e.g., meta-autunite (Merroun and Selenska-Pobell 2008; Krawczyk-Bärsch et al. 2015;

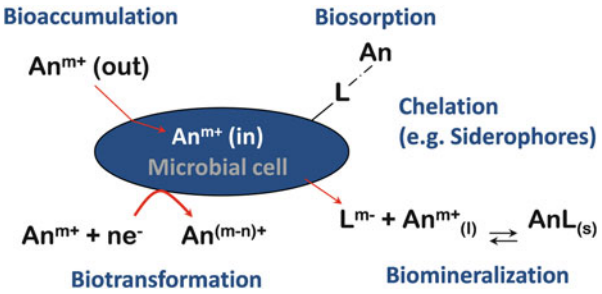

Fig. 1 Interaction mechanisms between microbes and actinides (An)

Reitz et al. 2014). Biotransformation is a very general term referring to a microbe-mediated conversion of the oxidation state (oxidation or reduction) of the respective An (Lovley et al. 1991; Panak and Nitsche 2001; Moll et al. 2006; Merroun and Selenska-Pobell 2008; Zhengji 2010; Kelly et al. 2010; Bernier-Latmani et al. 2010). Indirect interaction, for instance, by chelation, refers to the release of cellular ligands which bind to the An in solution. A prominent example is the release of siderophores of the pyoverdin type by *Pseudomonas fluorescens* which have shown to possess great binding potential toward U(VI), Cm(III), and Np (V) (Moll et al. 2008a, b, 2010). Our study is focused to broaden the knowledge concerning the bacterial diversity in Mont Terri Opalinus clay. After cultivation and characterization of dominant bacterial populations, we investigated their influence on the geochemical behavior of uranium and curium (Moll et al. 2013a).

2 Bacterial Diversity in Clay

For a long time, no in situ active life could be found in clay subsurface environments as potential host rocks for nuclear waste disposal, which seems to be unfavorable to microbial activity. However, the presence of bacteria in deep clay sediment of the Boom clay formation (Mol, Belgium) was shown in 1996 (Boivin-Jahns et al. 1996). In the Meuse/Haute-Marne Underground Research Laboratory located at Bure (300 km east of Paris), the Callovo–Oxfordian argillite formation was evaluated for its use as a potential host rock for a high-level radioactive waste repository in France (Cormenzana et al. 2008), and its microbial diversity was studied by culturing methods in Urios et al. (2012). The bacterial diversity found at the French formations was restricted to three bacterial phyla: *Firmicutes*, *Actinobacteria*, and *Proteobacteria* (Urios et al. 2013).

Over the last years, a couple of studies were performed about the microbial diversity in the Opalinus clay from the Mont Terri URL, Switzerland (Mauclaire et al. 2007; Stroes-Gascoyne et al. 2007; Poulain et al. 2008). Cultivation attempts and studies based on polar lipid fatty acid (PLFA) analyses suggested the presence of viable cells and detected PLFA biomarkers for Gram-negative bacteria and sulfate-reducing bacteria (in particular, *Desulfovibrio* spp., *Desulfobulbus* spp.,

and *Desulfobacter* spp.) in Opalinus clay (Mauclaire et al. 2007; Stroes-Gascoyne et al. 2007). Ribosomal RNA (rRNA) genes sequenced from enrichment cultures from Opalinus clay samples identified unknown species of *Sphingomonas* and *Alicyclobacillus* (Poulain et al. 2008). However, no PCR-amplifiable DNA from core samples could be extracted (Stroes-Gascoyne et al. 2007).

For the first time, DNA from Opalinus clay could be extracted in our laboratory by a method evolved by Selenska-Pobell and co-workers (Selenska-Pobell et al. 2001). This method combines a very effective direct lysis of microorganisms in environmental samples and the precipitation of the extracted DNA with polyethyleneglycol, with the final purification steps based on the use of AXG-100 cartridges (Macherey-Nagel, Düren, Germany). With this method, high molecular weight DNA from Opalinus clay of the Mont Terri URL was successfully isolated by using 50 g of sample material (Moll et al. 2013a). DNA from the inner part of the core and from the surface part of the core was extracted and analyzed. Ribosomal intergenic spacer analysis (RISA) patterns obtained from both samples did not match with each other, which indicated that the core surface was occupied by bacteria not or barely presented in the inner part of the core. A conclusion from this analysis is that clay material from the inner part of the core should be preferentially analyzed to avoid contaminants which might penetrate into the core during the sampling. An unexpected diverse bacterial community represented by five different bacterial phyla *Proteobacteria*, *Firmicutes*, *Bacteroidetes*, *Acidobacteria*, and *Actinobacteria* as well as unclassified bacteria was found in the inner part of the core by analyzing the 16S rRNA gene clone library (Moll et al. 2013a). The largest group in the sample includes rather diverse representatives of *Firmicutes*, which were affiliated with three distinct clostridial and one negativicutes family. The second largest group was, in contrast, more uniform and mainly represented by *Acidovorax* spp., belonging to the *betaproteobacterial* class of the phylum *Proteobacteria*. Their closest relatives were found in seafloor lavas from the East Pacific Rise (Santelli et al. 2008) and in Baltic Sea surface water (*Acidovorax* sp. C34). Representatives of *Acidovorax* are able to reduce nitrate, U (VI) to U(IV), and can couple the oxidation of ferrous iron (Fe(II)) with nitrate reduction (Nyman et al. 2006; Pantke et al. 2012; Carlson et al. 2013). The third predominant group was affiliated with *Bacteroidetes*, which are widely distributed in water, soils, and sediments and are characterized as a bacterial group which is very adaptive to changes in the nutrient conditions in the environment.

These results are in good agreement with previously performed multidisciplinary approaches to study the microbial diversity in Boom clay formation, a deep-subsurface clay deposit in Mol, Belgium (Wouters et al. 2013) and Spanish bentonites (Lopez-Fernandez et al. 2014, 2015). Wouters and colleagues confirmed the presence of a complex microbial community that can persist in subsurface Boom clay borehole water by using an integrated approach of microscopy, metagenomics, activity screening, and cultivation. Despite the presumed low-energy environment, microscopy and molecular analyses showed a large bacterial diversity and richness. Among different borehole water samples, the core bacterial community comprises seven bacterial phyla, namely, the

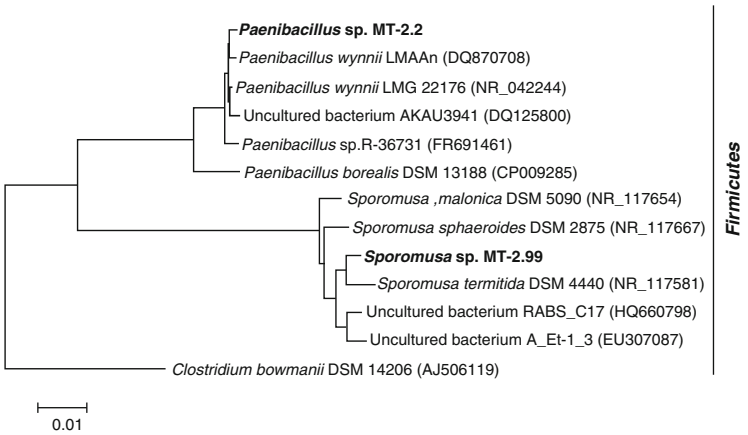

Fig. 2 Phylogenetic dendrogram of the 16S rRNA genes of isolates, obtained from the Mont Terri Opalinus clay sample MT-2 under anaerobic conditions on R2A agar plates

Proteobacteria, *Actinobacteria*, *Chlorobi*, *Firmicutes*, *Bacteroidetes*, *Chloroflexi*, and *Spirochaetes*. *Proteobacteria* made up of 76 % of the community, with the *Acidovorax* genus being highly prominent. In the Spanish bentonites, *Proteobacteria* and *Bacteroidetes* were dominant in clone libraries and Illumina sequencing approaches (Lopez-Fernandez et al. 2015). Culture-dependent analysis of microbial diversity from these clay formations was performed, and bacteria from different phyla were isolated as *Proteobacteria*, *Firmicutes*, and *Actinobacteria* (Lopez-Fernandez et al. 2014).

A culture-dependent approach was also performed in our laboratory with a sample from the inner part of the core from Mont Terri Opalinus clay by using R2A media (Moll et al. 2013a). The 16S rRNA genes of the isolates affiliated within the bacterial phylum *Firmicutes*. Interestingly, the 16S rRNA gene sequence of the isolate MT-2.99 was 96 % similar to the 16S rRNA gene sequences of *Sporomusa* spp. (*Sporomusa malonica* DSM 5090, *Sporomusa sphaeroides* DSM 2875, and *Sporomusa termitida* DSM 4440) (see Fig. 2); the uncultured bacterium clone A_Et-1_3 (EU307087), which was retrieved from Fe(III)-reducing enrichment culture (Hansel et al. 2008); and the uncultured bacterium RABS_C17, which was retrieved from an aquifer sediment where reductive immobilization of U took place (Sharp et al. 2011). *Sporomusa* spp. are obligatory anaerobic and sporulating bacteria (Kuhner et al. 1997). The 16S rRNA gene sequence of isolate MT-2.2 was 99 % similar with the 16S rRNA gene sequence of *Paenibacillus wynnii* LMAAn and *Paenibacillus wynnii* LMG 22176 T, which was found on Mars oasis on Alexander Island, Antarctica (Rodriguez-Diaz et al. 2005) (Fig. 2). Representatives of only one bacterial phylum could be isolated. This limited diversity could be interpreted with the unfavorable living conditions, characterizing the Opalinus clay. However, the capability of representatives of *Firmicutes* to form spores gives them a potential to survive in unfavorable conditions. On the other

Table 1 Protonation constants and site densities of Mont Terri Opalinus clay isolates determined by potentiometric titrations

Type of surface site	pK_a values		Site densities (mmol g^{-1} dry biomass)	
	Sporomusa sp. (Moll et al. 2013a)	*Paenibacillus* sp. (Lütke et al. 2013)	*Sporomusa* sp. (Moll et al. 2013a)	*Paenibacillus* sp. (Lütke et al. 2013)
Carboxyl	4.80 ± 0.06	4.90 ± 0.05	0.53 ± 0.08	0.55 ± 0.06
Phosphoryl	6.68 ± 0.06	6.66 ± 0.10	0.35 ± 0.03	0.24 ± 0.01
Amine/-OH	9.01 ± 0.08	9.20 ± 0.03	0.48 ± 0.05	1.20 ± 0.26

hand, only a small percentage of natural microbial populations can be isolated and studied in the laboratory due to the limited knowledge about their nutrient requirements and other life necessities (Stewart 2012).

The two isolates *Sporomusa* sp. MT-2.99 and *Paenibacillus* sp. MT-2.2 were chosen for further analyses to study how these isolates interact with U(VI) and Cm (III)/Eu(III). Potentiometric titration curves were recovered for the bacterial strains to characterize their cell surface functional groups. The potentiometric titration curves of the bacterial strains were all fitted with a three-site model using HYPERQUAD (Gans et al. 1996). The experimental details are described in detail in Lütke (2013), Lütke et al. (2013), and Moll et al. (2013a, b).

The description of the bacterial cell wall with three major global binding sites is a common approach (Fein et al. 1997; Yee et al. 2004; Dittrich and Sibler 2005; Fang et al. 2009). By comparing the determined values (Table 1) to the pK_a ranges of different bacterial functional groups reported in, e.g., Cox et al. (1999), the respective surface functional groups can be attributed to carboxyl, phosphate, and amine moieties. The determined pK_a values of the major global binding sites are in a very good agreement to those determined for a strain of the Gram-negative genus *Calothrix* (Yee et al. 2004). Our experiments showed that the major surface functional groups of both strains have similar pK_a values, whereas a higher variation could be found in the respective site densities. Both parameter the pK_a values and corresponding site density are necessary to elucidate the An speciation in the presence of these bacteria in terms of surface complexation constants to be used in modeling codes.

3 Determination of Actinide Interactions with Mont Terri Opalinus Clay Isolates

In the following sections of the chapter, the unique potential of bacteria to influence the aqueous speciation of uranium(VI) and curium(III) will be highlighted. The diversity of interaction mechanisms is due to the variety of metabolism and cell surface structures among microbes. The cell walls of bacteria represent a highly efficient matrix for metal sorption offering mainly carboxylic, phosphoryl, and amine moieties for metal complexation (Beveridge and Doyle 1989). It has been

proposed that bacteria freely suspended in solution may even have a radionuclide-sorbing capacity higher than that of the surrounding mineral phases (Pedersen and Albinsson 1992; Bencheikh-Latmani et al. 2003; Ohnuki et al. 2005). The composition of the cell wall differs for Gram-negative and Gram-positive bacterial strains. Since strains of the genera *Sporomusa* and *Paenibacillus* differ by that, with the present work, the influence of the cell wall structure on actinide binding can be assessed. The cell walls of Gram-negative bacteria possess an outer membrane of lipopolysaccharide (LPS), a periplasm consisting of a thin layer of peptidoglycan (PG), and an inner cytoplasmic membrane (phospholipid bilayer). The LPS offers carboxyl, phosphoryl, hydroxyl, and amino groups as binding sites for metals (Barkleit et al. 2008). The PG polymeric framework itself is rich in carboxylate groups. In the PG framework, teichoic (basically glycerol phosphate polymers) and teichuronic acids are interconnected, which contain also phosphate groups. The strain *Sporomusa* sp. MT-2.99 showed a Gram-negative staining (Moll et al. 2013a). The *Selenomonas–Megasphaera–Sporomusa* branch unifies members of the *Firmicutes* with Gram-negative-type cell envelopes but still belongs to *Clostridia* (Yutin and Galperin 2013). In contrast to the genus *Sporomusa*, the genus *Paenibacillus* is Gram-positive. In Gram-positive bacteria, the major and very outer cell wall component is PG, which can make up to 90 % of the dry weight of the bacterial cells (Voet et al. 2002).

The thermodynamic data of U(VI) species formed at the bacterial surface were determined with potentiometric titration. Moreover, we assessed the U(VI) and Cm (III) speciation at the cell surface using time-resolved laser-induced fluorescence spectroscopy (TRLFS) as a direct speciation technique. In selected experiments, europium(III) as a nonradioactive analogue for An(III) was used also to validate the Cm(III) TRLFS speciation results by potentiometric titration and also by TRLFS. In Moll et al. (2013a, 2014), we could show that Eu(III) can be used as a nonradioactive analogue to mimic bacterial interactions of An(III). TRLFS has been proven in the past to be a powerful tool especially useful for the determination of the uranium, curium, and europium speciation at low, environmentally relevant concentrations (Geipel 2006; Lütke et al. 2012, 2013; Moll et al. 2014). Furthermore, results on the influence of $[U(VI)]_{initial}$ and pH on the quantities of U(VI) bound and on the bacteria-mediated inorganic phosphate liberation by *Paenibacillus* sp. are presented.

3.1 U(VI) Interaction Studies with Paenibacillus *sp. and* Sporomusa *sp. Cells*

3.1.1 U(VI) Binding by *Paenibacillus* sp. and *Sporomusa* sp. cells as a Function of [U(VI)] and pH Including the Bacteria-Mediated Inorganic Phosphate Release (Lütke et al. 2013; Moll et al. 2013a)

The biosorption efficiency of microbial strains is a key parameter for judging the retardation of the respective actinide caused by the strain. As depicted in Fig. 3,

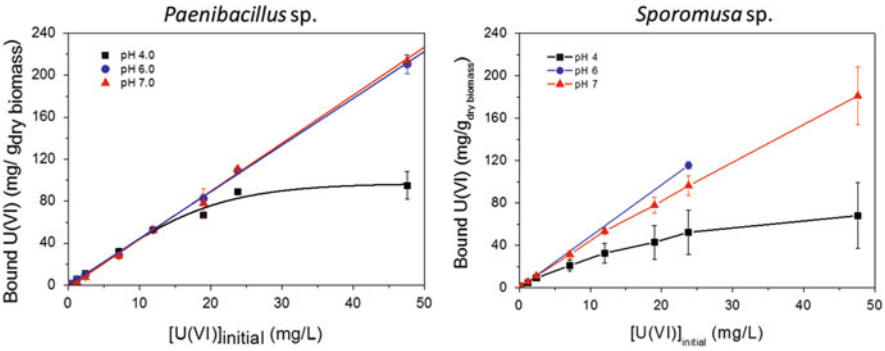

Fig. 3 U(VI) binding onto *Paenibacillus* sp. (left) and *Sporomusa* sp. cells in dependence on $[UO_2^{2+}]_{initial}$ at different pH values in 0.1 M $NaClO_4$, [dry biomass] = 0.2 gL^{-1}

Paenibacillus sp. and *Sporomusa* sp. cells display a strong pH-dependent affinity for U(VI). At both pH values 6 and 7 and an initial [U(VI)] of about 48 mg L^{-1}, more than two times as much U(VI) is bound as at pH 4 for *Paenibacillus* sp. (Lütke et al. 2013). Under similar conditions, almost three times as much as U(VI) is immobilized for *Sporomusa* sp. (Moll et al. 2013a). Interestingly, for pH 6 and 7, the dependency of the sorption on the initial [U(VI)] can be described in both cases by a linear correlation, and almost identical sorption efficiencies were found. At pH 4 on the contrary, the sorption shows an asymptotic behavior with increasing $[U(VI)]_{initial}$. This finding can possibly be explained by a smaller degree of deprotonation of the cell surface functional groups at pH 4 in comparison to pH 6 or 7 resulting in a fewer number of functional groups available for U (VI) complexation.

It has been discovered very early that the release of phosphate can be an active microbial process and altered through external conditions (Shapiro 1967). We could show that the dependency of the inorganic phosphate release by *Paenibacillus* sp. cells depends on the initial U(VI) concentration and pH. The phosphatase activity is maximum (4.8 mg L^{-1}) at pH 6. A pH-dependent bacterial phosphatase activity was also observed for another *Paenibacillus* strain, *Paenibacillus* sp. - JG-TB8 (Reitz et al. 2014), which increased drastically from pH 3 to 6, having maximum activity also at pH 6. At a [U(VI)] as low as 5×10^{-6} M, inorganic phosphate liberation is already markedly decreased in comparison to the samples without any U(VI) added (3.8 mg L^{-1} at pH 6). This effect is strongest at pH 4. The decrease of inorganic phosphate release as response to U(VI) contact was also found for a strain of *P. fluorescens* (Lütke et al. 2012). Upon increasing $[U(VI)]_{initial}$, the phosphate decrease becomes more drastic. Inorganic phosphate release by *Sporomusa* sp. could be also proven. U(VI) phosphate complexes give characteristic luminescence spectra. Thus, the release of inorganic phosphate into the cell supernatants should be observable with TRLFS as described later on.

3.1.2 U(VI) Speciation Explored by Potentiometric Titration (Lütke et al. 2013; Moll et al. 2013a)

The titration data of bacterial cells and UO_2^{2+} were fitted by including the following hydrolytic uranyl species and their stability constants: $(UO_2)_2(OH)_2^{2+}$, $(UO_2)_3(OH)_5^{+}$, and $(UO_2)_4(OH)_7^{+}$(Guillaumont et al. 2003). The titration curves could be modeled with a very good fit result when the bacterial surface complexes R–COO–UO_2^{+}, R–O–PO_3H–UO_2^{+}, R–O–PO_3–UO_2, and (R–O–PO_3)$_2$–UO_2^{2-} were considered. The respective calculated stability constants are summarized in Table 2.

From the stability constants listed in Table 2, it can be seen that overall U (VI) can form fairly stable complexes with the surface functional groups of *Paenibacillus* sp. and *Sporomusa* sp. cells. Furthermore, the interaction with phosphoryl sites is characterized by stability constants several orders of magnitude greater than that of carboxyl site interaction. Our reported stability constant of the *Paenibacillus* sp. R–COO–UO_2^{+} complex is in very good agreement with the stability constant of the 1:1 complex of U(VI) interacting with carboxylic groups of the *Bacillus subtilis* cell surface, log $\beta_{110} = 5.4 \pm 0.2$, published by Fowle et al. (2000). If compared to the results published by Barkleit et al. (2008, 2009) on the U(VI) interaction with PG (R–COO–UO_2^{+} with a log β value of 4.02 was specifically attributed to UO_2^{2+} interacting with glutamic acid groups; R–COO–UO_2^{+} with a log β value of 7.28 was specifically attributed to UO_2^{2+} interacting with diaminopimelic acid groups) and LPS (R–COO–UO_2^{+} with a log β value of 5.93), deviate somewhat from our results. However, it shows the relatively broad range of log β values of U(VI) complexes with carboxyl groups in biological systems. If compared to the results in Table 2 gained with the Äspö isolate *P. fluorescens* (Gram-negative), it becomes obvious that although the same

Table 2 Calculated stability constants of UO_2^{2+}/Eu^{3+}/Cm^{3+} complexes with surface functional groups of *Paenibacillus* sp. and *Sporomusa* sp. cells determined by potentiometric titration (Lütke et al. 2013; Moll et al. 2013a, 2014)

Complex	xyz[a]	log β_{xyz} (±SD) *Paenibacillus* sp.	log β_{xyz} (±SD) *Sporomusa* sp.
R–COO–UO_2^{+}	110	5.33 ± 0.08	4.75 ± 0.98
R–O–PO_3–UO_2	110	8.89 ± 0.04	8.58 ± 0.04
R–O–PO_3H–UO_2^{+}	111	12.92 ± 0.05	13.07 ± 0.06
(R–O–PO_3)$_2$–UO_2^{2-}	120	13.62 ± 0.08	13.30 ± 0.09
R–COO–Eu^{2+}	110	5.70 ± 0.25	6.89 ± 0.62
R–O–PO_3–Eu^{+}	110		7.71 ± 0.33
R–O–PO_3H–Eu^{2+}	111	13.64 ± 0.30	15.49 ± 0.19
R–COO–Cm^{2+}	110		8.06 ± 0.61[b]
R–O–PO_3–Cm^{+}	110		
R–O–PO_3H–Cm^{2+}	111	13.94 ± 0.18[b]	13.90 ± 0.90[b]

[a]Stoichiometry of metal–ligand–H
[b]From TRLFS

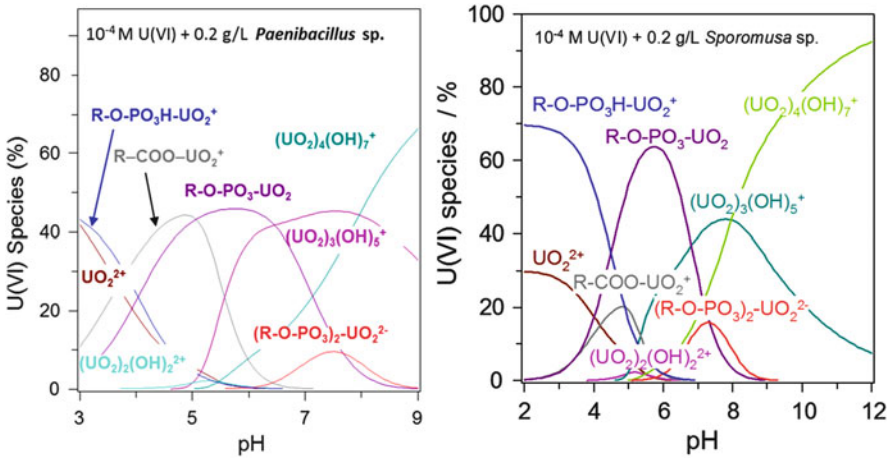

Fig. 4 U(VI) species distributions in the presence of *Paenibacillus* sp. and *Sporomusa* sp. cells in dependence on pH: [U(VI)] = 1 × 10^{-4} M, [dry biomass] = 0.2 gL^{-1}. CO_2-free system

complex stoichiometries could be fitted to the titration data (Lütke et al. 2012), the gained stability constants of the R–COO–UO_2^+ complex displayed a range of 4.75–6.66, indicating the dependency of those on the individual cell wall structure. The comparison of the determined stability constants for phosphoryl interaction, in specific of the R–O–PO_3H–UO_2^+ complex of both strains, to the literature, revealed again a fairly good agreement with the result gained by Fowle et al. (2000) (*B. subtilis*: log β = 11.8) and Barkleit et al. (2008) (LPS: log β = 11.66). An agreement to the literature was observed when comparing the results on U (VI) interaction with deprotonated bacterial phosphoryl sites to the results gained with the model compound LPS (Barkleit et al. 2008: log β_{110} = 7.50 and log β_{120} = 13.80). This might suggest that LPS is a good representative of the phosphoryl properties of the bacterial cell envelope in terms of their binding characteristics toward U(VI).

The discussion of the determined bacterial U(VI) surface complexation constants (Table 2) is illustrated by U(VI) species distribution calculations using the software HySS2009 (Alderighi et al. 1999). The U(VI) speciation in the acidic pH range (pH 3) is determined majorly by UO_2^{2+} being coordinated to hydrogen phosphoryl sites (Fig. 4). This finding coheres well to what was reported by Fowle et al. (2000): the best fit of data obtained from U(VI) binding to *B. subtilis* was achieved by considering U(VI) bound via H-phosphoryl groups at low pH. Nevertheless, at pH 3, for instance, there is a portion of noncomplexed U (VI) in the cell supernatant, which should be detectable using TRLFS.

The species distribution diagram furthermore shows that upon increasing pH, an increasing coordination of UO_2^{2+} to carboxylic and deprotonated phosphoryl sites occurs. Due to the lower stability of the carboxyl bound U(VI) complex in the *Sporomusa* sp. system, here, phosphoryl bound U(VI) dominates compared to

Paenibacillus sp. At a pH greater than 7, uranyl hydroxides dominate the speciation in a CO_2-free system.

3.1.3 U(VI) Speciation Explored by Time-Resolved Laser-Induced Fluorescence Spectroscopy (TRLFS) in the *Paenibacillus* sp. System (Lütke et al. 2013; Moll et al. 2013a)

From both, the cells and the according cell supernatants at pH 4 and 7, U (VI) luminescence spectra were collected and compared (Fig. 5a).

While the band positions of the static spectra give indications for possible U (VI) surface species formed, the time-resolved measurements give insight into the number of present luminescent species. A detailed summary of luminescence emission maxima and calculated lifetimes related to the spectra discussed including the comparison to the appropriate literature is given in Lütke et al. (2013). Also TRLFS affirmed (Fig. 5a) that the speciation at the cell surface changes in dependence on the pH. With a pH shift from 4 to 7, the main luminescence emission band is slightly redshifted by roughly 3 nm, and also the spectral pattern changes. The emission maxima of U(VI) in the supernatant at pH 4 indicate the occurrence of at least two luminescent species having quite distinct emission maxima. An emission band located at 509.7 nm and the associated lifetime of 1.03 ± 0.02 µs clearly indicate a spectral contribution of the free UO_2^{2+} ion. The second spectral feature of U(VI) in the cell supernatant at pH 4 is quite similar to the spectrum of U(VI) in the supernatant at pH 7 in terms of the position of the main luminescence emission band, indicating the presence of a similar species at both pH values. This gives evidence for a cellular ligand being released which coordinates strongly to U(VI); otherwise, the spectral pattern would show a strong pH dependency due to the increasing formation of uranyl hydroxides with increasing pH. Considering also the

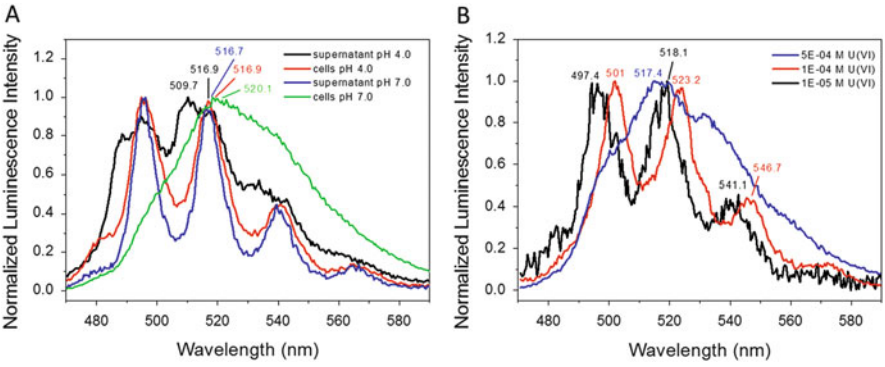

Fig. 5 (**a**) Luminescence spectra of U(VI)-loaded *Paenibacillus* sp. cells and U(VI) in the cell supernatants at pH 4 and 7 in 0.1 M $NaClO_4$ ($[U(VI)]_{initial}$ 1×10^{-4} M, [dry biomass] 0.2 gL^{-1}). (**b**) Luminescence spectra of U(VI)-loaded *Paenibacillus* sp. cells with variation of $[U(VI)]_{initial}$ and at pH 5 in 0.1 M $NaClO_4$, [dry biomass] = 0.2 gL^{-1}

relatively sharp emission bands and the position of the emission maxima of U (VI) in the supernatant at pH 7, the presence of pure U(VI) hydroxide can be excluded. Comparing these band positions to those of model compounds of the literature, especially those of UO_2^{2+} coordinated by $H_2PO_4^-$ and HPO_4^{2-} (Panak et al. 2000), a coordination by inorganic phosphate seems probable. Since inorganic phosphate was already proven to be released into the supernatants in significant amounts by means of ion exchange chromatography, a coordination of UO_2^{2+} by inorganic phosphate seems likely. Comparing the spectrum of U(VI) bound to the cells at pH 4 to that at pH 7, a redshift of 3.2 nm occurs. This significant redshift is in agreement to what was predicted in the calculated U(VI) species distribution. The U(VI) species distribution had shown the increased formation of UO_2^{2+} complexes with deprotonated phosphoryl sites in the neutral pH range, while at low pH around pH 4, uranyl is predominantly coordinated via H-phosphoryl and carboxylic sites. This dependency had also been reported by Barkleit et al. (2008), investigating the interaction of LPS with U(VI). A redshift of the emission maxima occurred when going from UO_2^{2+} complexed by protonated phosphoryl to deprotonated phosphoryl sites. Besides the position of the luminescence emission maxima, also the luminescence lifetimes can be helpful to identify the present species. At pH 4 for U(VI) bound to the cells, two lifetimes could be determined: 0.66 and 2.69 µs. For pH 7, also two lifetimes were found: 0.53 and 2.34 µs. To discriminate here between carboxyl and phosphoryl, and potentially even between deprotonated phosphoryl and H-phosphoryl, a measurement at pH 5 in dependency on $[U(VI)]_{initial}$ was carried out in order to attribute the lifetimes to present U (VI) species (Fig. 5b). In case of a deficit of [U(VI)] compared to the [surface sites], U(VI) should be bound at first via protonated phosphoryl sites. With increasing [U (VI)], an increased amount of R–O–PO_3–UO_2 would be formed. If [U(VI)] is increased further, finally, the carboxyl groups as weakest ligand according to the determined stability constants and in accordance to many exemplary cases in the literature (Fowle et al. 2000; Barkleit et al. 2008; Rothstein 1962) will be covered by U(VI). As depicted in Fig. 5b, a significant redshift of about 5 nm occurs at an increased [U(VI)] of 1×10^{-4} M compared to the spectrum at the smallest investigated [U(VI)] of $1 \times \cdot 10^{-5}$ M. The luminescence emission maxima of this spectrum point strongly toward a uranyl phosphoryl interaction (see for comparison Günther et al. 2006). The spectrum at $[U(VI)]_{initial} = 1 \times 10^{-4}$ M accompanied by a short lifetime of in average 0.55 µs can clearly be assigned to phosphoryl-bound U (VI), most likely to deprotonated phosphoryl (R–O–PO_3–UO_2). If the [U(VI)] is increased further, the main emission band shifts toward shorter wavelength even below the position of the main emission maximum of the spectrum of the lowest measured [U(VI)]. This finding as well as the spectral pattern observed at this [U (VI)] gives indications for a formation of polynuclear U(VI) species. The data evaluation showed that both species, the R–O–PO_3H–UO_2^+ and the (R–O–PO_3)$_2$–UO_2^{2-} complex, have similar lifetimes and longer than that of the R–O–PO_3–UO_2 complex. Similar observations were made by Barkleit et al. (2008) for UO_2^{2+}–LPS complexes. In the U(VI)–*Sporomusa* sp. system, the major contribution of phosphoryl sites on U(VI) speciation could be also confirmed by preliminary TRLFS

measurements. TRLFS as a direct speciation technique could successfully prove the following: the pH-dependent cell-mediated inorganic phosphate release, the occurrence of free UO_2^{2+} at acidic pH as predicted by the calculated U(VI) speciation, and the occurrence of different UO_2^{2+} phosphoryl species.

3.2 *Cm(III) Interaction Studies with* Paenibacillus *sp. and* Sporomusa *sp. Cells (Lütke 2013; Moll et al. 2013a, 2014)*

In the following paragraph, the change of the Cm^{3+} speciation in the presence of *Sporomusa* sp. cells using TRLFS will be highlighted and compared to findings in the *Paenibacillus* sp. system. For a detailed description of the ongoing process, please refer to the corresponding literature (Lütke 2013; Moll et al. 2013a, 2014).

In the presence of *Sporomusa* sp. cells, a strong decrease in the emission band of the free Cm^{3+} at 593.8 nm could be detected already at pH 1.95 (Fig. 6a). A new redshifted emission band at around 600 nm occurred simultaneously showing the influence of a first Cm^{3+}–*Sporomusa* sp. species. It demonstrates that *Sporomusa* sp. interacts with curium(III) from acidic solutions. The dependencies found in the TRLFS spectra suggested the occurrence of two individual Cm^{3+}–*Sporomusa* sp. species between pH 1.9 and 8.1 having emission maxima at ca. 600 and 601.4 nm. The pH-dependent change of the emission data of the Cm^{3+}–*Sporomusa* sp. system implies the involvement of two functional groups located at the cell envelope structure.

In all bacterial samples, a bi-exponential luminescence decay behavior was measured. The averaged value of the shorter lifetime was calculated to be 108 ± 15 µs, whereas the component with the longer lifetime was calculated to be

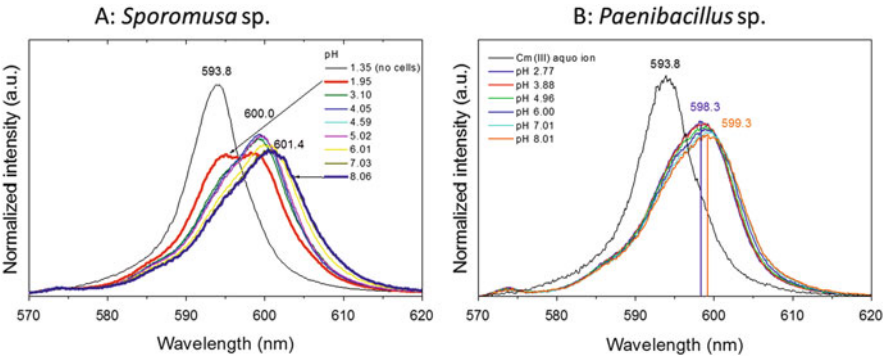

Fig. 6 Luminescence emission spectra of 0.3 µM curium(III) in 0.1 M $NaClO_4$ as a function of pH: (**a**) measured at a fixed *Sporomusa* sp. concentration of 0.02 $g_{dry\ weight}L^{-1}$ and (**b**) measured at a fixed *Paenibacillus* sp. concentration of 0.2 $g_{dryweight}L^{-1}$

252 ± 46 μs. Using the empirical equation given by Kimura and Choppin (1994), these lifetimes correspond to 5.0 and 2.0, respectively, remaining water molecules in the curium(III) first coordination sphere. In general, we found a stronger contribution of the long lifetime to measured sum lifetimes in the acidic pH region. In contrast, the short lifetime contributed most in the neutral to alkaline pH region. Due to these findings and by comparison to relevant literature values (see Moll et al. 2014), the longer lifetime can be assigned to Cm^{3+}–*Sporomusa* sp. species formed in the acidic pH region (phosphoryl interaction), whereas the shorter lifetime corresponds to Cm^{3+}–*Sporomusa* sp. species formed in the neutral to alkaline pH region (carboxyl interaction).

For *Sporomusa* sp., the interaction mechanism with Cm(III) and also Eu(III) is dominated by a major process a reversible biosorption reaction. However, we could identify a certain amount, ca. 30 %, which is irreversibly bound to the cells. This minor process can be described by an immobilization of Cm(III)/Eu(III) within the complex cell envelope structure of *Sporomusa* sp.

The program SPECFIT (Binstead et al. 2004) was used to extract the bacterial curium(III) surface complexation constants (Table 2) and the corresponding single component spectra. The calculation procedure is based on the formal complex formation equation for discrete binding sites and the appropriate mass action law, which represents the complex stability constant log β_{xyz}. The variations observed in the emission data (e.g., shown in Fig. 6a) could be described by the formation of two curium(III) surface complexes. The best fits were obtained with two 1:1 complexes, $R-O-PO_3H-Cm^{2+}$ (Cm^{3+}–*Sporomusa* sp. species 1) and $R-COO-Cm^{2+}$ (Cm^{3+}–*Sporomusa* sp. species 2). The surface complexation constants were calculated to be log $\beta_{111} = 13.90 \pm 0.90$ for the protonated phosphoryl complex and log $\beta_{110} = 8.06 \pm 0.61$ for the carboxyl coordination.

We were able to identify a Eu(III) surface complex with deprotonated phosphoryl groups, $R-O-PO_3-Eu^{+}$, by potentiometric titration in the *Sporomusa* sp. system. Both species $R-COO-Eu^{2+}$ and $R-O-PO_3-Eu^{+}$ coexist between pH 4 and 8. Here, we could see the limitations of TRLFS. A differentiation of two individual species was not possible in this pH range in the spectroscopic titrations by TRLFS. It follows that the stability range of Cm(III)/Eu(III) carboxyl interactions might be overdetermined by TRLFS at least for the *Sporomusa* sp. system.

From Fig. 6b, it becomes obvious that the luminescence spectrum of Cm(III) in the presence of *Paenibacillus* sp. cells is also redshifted compared to that of the Cm (III) aquo ion by approximately 5 nm indicating complex formation. In contrast to the *Sporomusa* sp. system, the spectra of Cm(III) in the presence of the *Paenibacillus* sp. cells undergo only a slight redshift of about 1 nm within pH 3–8. The complex $R–O–PO_3H–Cm^{2+}$ could be extracted having a stability constant log β of 13.94 ± 0.18 using SPECFIT. Obviously, Cm(III) displays high affinity to the phosphoryl sites of the *Paenibacillus* sp. cell surface. No carboxyl interaction could be detected by TRLFS. Investigating the interaction of *Paenibacillus* sp. cells with Eu(III) using potentiometry, a comparatively small stability constant was found for the $R–COO–Eu^{2+}$ complex (Table 2). Taking this into consideration

and additionally that the corresponding Cm(III) complex might possess a lower luminescence quantum yield than the corresponding Cm(III) complex with carboxyl sites of *Sporomusa* sp., the failure of detecting a Cm(III) carboxyl complex with *Paenibacillus* sp. cells by TRLFS might be explainable.

Over the whole investigated pH region, two luminescence lifetimes were detected in the *Paenibacillus* sp. system: $\tau_1 = 238 \pm 23$ µs and $\tau_2 = 477 \pm 73$ µs. From both detected lifetimes in the bacterial Cm(III) suspensions at all investigated pH values, the longer lifetime can be clearly assigned to the cell-bound Cm(III). This implies that only one type of functional group is involved in complex formation over the whole investigated pH region. As consequence, the lifetime of in average 238 ± 23 µs belongs to a Cm(III) species in the aqueous phase. At pH 3, hardly any Cm(III) emission decay could be detected due to the low [Cm(III)] remaining in solution after sorption to the biomass. Hence, at pH 3, 95 % Cm(III) was bound, while in the neutral pH range, only 4 % Cm(III) was accumulated due to phosphate release. Therefore, in the presence of Cm(III), *Paenibacillus* sp. cells displayed a pronounced phosphatase activity which was strongly pH-dependent. At pH 8, the time-resolved measurements of the supernatant after 24 h Cm(III) contact revealed two luminescence lifetimes: 183 ± 46 µs and 327 ± 19 µs. The first one might indicate the formation of Cm(III) phosphate, while the second one implies complexation by functional groups of organic origin. Possibly, the second lifetime is attributable to Cm(III) being complexed by cell-released matter. Extraction studies with EDTA showed that binding was completely reversible indicating a pure biosorption process to the cell envelope. In summary and to propose an overall model for Cm(III) interaction with *Paenibacillus* sp. cells affecting the Cm(III) speciation, e.g., at pH 3, Cm(III) initially is present in solution solely as the Cm(III) aqua ion. As such, it must adhere well to the cell surfaces since 95 % Cm(III) gets immobilized, although remarkable cell-mediated phosphate release occurs. It was shown that Cm(III) forms primarily the complex R–O–PO_3H–Cm^{2+} at the cell envelope. At pH 3, in minor amounts, $CmHPO_4^+$ and $CmH_2PO_4^{2+}$ coexist with the cell-bound Cm^{3+}. At pH 8, compared to pH 3, the amounts of cell-bound Cm (III) and $CmHPO_4^+$/$CmH_2PO_4^{2+}$ are reversed.

4 Summary and Conclusions

The major aim of our study was to assess the U(VI) and Cm(III) complexation by the bacterial surface functional groups of *Sporomusa* sp. MT-2.99 and *Paenibacillus* sp. MT-2.2 on a molecular level to provide stability constants. Within the investigated pH range (2–8), carboxyl and phosphoryl moieties of the bacterial cell envelope are responsible for An/Ln binding. To detect and characterize the relevant U(VI)/Eu(III)/Cm(III) surface complexes, TRLFS as a direct speciation technique in combination with potentiometric titration for U(VI) and Eu(III) was applied. It could be demonstrated that both methods can complement each other.

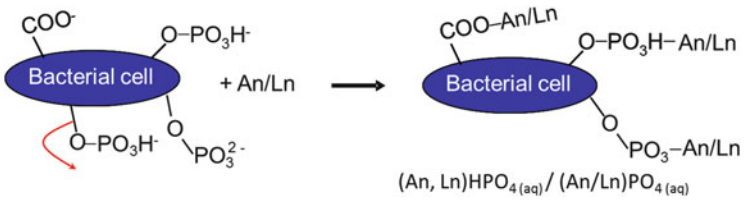

Fig. 7 Simplified scheme of impact of bacterial cells on An/Ln speciation at anaerobic conditions

In view of the versatile possible interaction mechanisms between bacteria and An/Ln, it was found that both strains display indirect interaction in the form of a pronounced pH- and [An]-dependent phosphatase activity and concomitant phosphate release, which was, for example, highest at pH 6 for *Paenibacillus* sp. Using TRLFS, it was proven that phosphate was released into the medium and binds dissolved U(VI).

Using potentiometry for both bacterial species, the following U(VI) surface complexes and their stability constants were determined: R–COO–UO_2^+, R–O–PO_3H–UO_2^+, R–O–PO_3–UO_2, and (R–O–PO_3)$_2$–UO_2^{2-}. Overall, for all strains, the following order of stability can be established for the U(VI) complexes formed at the bacterial cell surfaces: (R–O–PO_3)$_2$–UO_2^{2-} > R–O–PO_3H–UO_2^+ > R–O–PO_3–UO_2 > R–COO–UO_2^+.

In the *Sporomusa* sp. system, the surface species R–COO–Cm^{2+} and R–O–PO_3H–Cm^{2+} could be characterized spectroscopically by TRLFS. For Eu(III) with the bacterial isolates, the surface species R–COO–Eu^{2+} and R–O–PO_3H–Eu^{2+} were identified and characterized thermodynamically. Only in the *Sporomusa* sp. system, a Eu(III) surface complex with deprotonated phosphoryl groups, R–O–PO_3–Eu^+, could be identified by potentiometric titration. Eu(III) can be used as a nonradioactive analogue to mimic bacterial interactions of An(III). TRLFS studies on the interaction of Cm(III) with *Paenibacillus* sp. revealed that Cm(III) is solely bound by the bacterial phosphoryl moieties. The presence of the R–O–PO_3H–Cm^{2+} species over a wide pH range could be demonstrated. Although the existence of a Eu(III) species with carboxylic groups at pH 8 was predicted, no such Cm(III) species could be detected at that pH using TRLFS.

Our results suggested that U(VI)/Eu(III)/Cm(III) complexes with the surface functional groups of the *Sporomusa* sp. and *Paenibacillus* sp. cell envelope dominate their respective speciation over a broad pH and biomass concentration range. To summarize, the following simplified overall schema of the impact of bacterial strains on U(VI), Eu(III), and Cm(III) speciation is proposed (Fig. 7).

In conclusion, Mont Terri Opalinus clay contains a rather diverse bacterial community of representatives of *Proteobacteria*, *Firmicutes*, *Bacteroidetes*, *Acidobacteria*, and *Actinobacteria* as well as unclassified bacteria. However, only representatives of *Firmicutes* could be isolated, namely, *Sporomusa* sp. MT-2.99 and *Paenibacillus* sp. MT-2.2. The isolated Mont Terri Opalinus clay isolates may influence the speciation and hence the migration behavior of selected An/Ln under environmental conditions. The stability constants presented are valuable for

modeling the U(VI), Eu(III), and Cm(III) speciation and distribution in the environment. Hence, the results contribute to better estimating the safety of a planned nuclear waste deposition site.

Further studies could focus on the metabolic activity of indigenous microbes in geological formations foreseen for a save storage of nuclear waste. The metabolic activity can affect the physical and geochemical conditions of a geologic repository and hence the speciation of accidentally released An. The quantification of the total microbial DNA in terms of cell numbers in pore waters and cores, for instance, as a function of depth should be addressed further. The performed laboratory experiments in this study could be extended to more environmental conditions (e.g., ternary systems containing the host rock—microbial cells—metals). All this would complete our knowledge of microbial processes influencing the fate of accidentally released An and fission products in the environment.

Acknowledgments The authors thank the BMWi for financial support (contract nos.: 02E10618 and 02E10971), Velina Bachvarova and Sonja Selenska-Pobell for microbial diversity analysis and isolation of the bacteria, Monika Dudek for cultivation of the bacteria, as well as the BGR for providing the clay samples. The authors are indebted to the US Department of Energy, Office of Basic Energy Sciences, for the use of ^{248}Cm via the transplutonium element production facilities at Oak Ridge National Laboratory; ^{248}Cm was made available as part of collaboration between HZDR and the Lawrence Berkeley National Laboratory (LBNL).

References

Alderighi L, Gans P, Ienco A, Peters D, Sabatini A, Vacca A (1999) Hyperquad simulation and speciation (HySS): a utility program for the investigation of equilibria involving soluble and partially soluble species. Coord Chem Rev 184:311–318

Anderson C, Johnsson A, Moll H, Pedersen K (2011) Radionuclide geomicrobiology of the deep biosphere. Geomicrobiol J 28:540–561

Barkleit A, Moll H, Bernhard G (2008) Interaction of uranium(VI) with lipopolysaccharide. Dalton Trans 21:2879–2886

Barkleit A, Moll H, Bernhard G (2009) Complexation of uranium(VI) with peptidoglycan. Dalton Trans 27:5379–5385

Bencheikh-Latmani R, Leckie JO, Bargar JR (2003) Fate of uranyl in a quaternary system composed of uranyl, citrate, goethite, and *Pseudomonas fluorescens*. Environ Sci Technol 37:3555–3559

Bernier-Latmani R, Veeramani H, Vecchia ED, Junier P, Lezama-Pacheco JS, Suvorova EI, Sharp JO, Wigginton NS, Bargar JR (2010) Non-uraninite products of microbial U(VI) reduction. Environ Sci Technol 44:9456–9462

Beveridge TJ, Doyle RJ (1989) Metal ions and bacteria. Wiley, New York

Binstead RA, Zuberbühler AD, Jung B (2004) SPECFIT global analysis system version 3.0.35

Boivin-Jahns V, Ruimy R, Bianchi A, Daumas S, Christen R (1996) Bacterial diversity in a deep-subsurface clay environment. Appl Environ Microbiol 62:3405–3412

Brockmann S, Arnold T, Bernhard G (2014) Speciation of bioaccumulated uranium(VI) by *Euglena mutabilis* cells obtained by laser fluorescence spectroscopy. Radiochim Acta 102:411–422

Brookshaw DR, Pattrick RAD, Lloyd JR, Vaughan DJ (2012) Microbial effects on mineral-radionuclide interactions and radionuclide solid-phase capture processes. Mineral Mag 76:777–806

Carlson HK, Clark IC, Blazewicz SJ, Iavarone AT, Coates JD (2013) Fe(II) oxidation is an innate capability of nitrate-reducing bacteria that involves abiotic and biotic reactions. J Bacteriol 195:3260–3268

Cormenzana JL, García-Gutiérrez M, Missana T, Alonso U (2008) Modelling large-scale laboratory HTO and strontium diffusion experiments in Mont Terri and Bure clay rocks. Phys Chem Earth 33:949–956

Cox JS, Smith DS, Warren LA, Ferris FG (1999) Characterizing heterogeneous bacterial surface functional groups using discrete affinity spectra for proton binding. Environ Sci Technol 33:4514–4521

Dittrich M, Sibler S (2005) Cell surface groups of two picocyanobacteria strains studied by zeta potential investigations, potentiometric titration, and infrared spectroscopy. J Colloid Interface Sci 286:487–495

Fang L, Cai P, Chen W, Liang W, Hong Z, Huang Q (2009) Impact of cell wall structure on the behaviour of bacterial cells in the binding of copper and cadmium. Colloids Surf A 347:50–55

Fein JB, Daughney CJ, Yee N, Davis TA (1997) A chemical equilibrium model for metal adsorption onto bacterial surfaces. Geochim Cosmochim Acta 61:3319–3328

Fowle DA, Fein JB, Martin AM (2000) Experimental study of uranyl adsorption onto *Bacillus subtilis*. Environ Sci Technol 34:3737–3741

Gans P, Sabatini A, Vacca A (1996) Investigation of equilibria in solution. Determination of equilibrium constants with the HYPERQUAD suite of programs. Talanta 43:1739–1753

Geipel G (2006) Some aspects of actinide speciation by laser-induced spectroscopy. Coord Chem Rev 250:844–854

Guillaumont R, Fanghänel T, Fuger J, Grenthe I, Neck V, Palmer DA, Rand MH (2003) Update on the chemical thermodynamics of uranium, neptunium, plutonium, americium and technetium. OECD/NEA, Paris

Günther A, Geipel G, Bernhard G (2006) Complex formation of U(VI) with the amino acid L-threonine and the corresponding phosphate ester O-phospho-L-threonine. Radiochim Acta 94:845–851

Günther A, Raff J, Merroun ML, Roßberg A, Kothe E, Bernhard G (2014) Interaction of U (VI) with Schizophyllum commune studied by microscopic and spectroscopic methods. Biometals 27:775–785

Hansel CM, Fendorf S, Jardine PM, Francis CA (2008) Changes in bacterial and archaeal community structure and functional diversity along geochemically variable soil profile. Appl Environ Microbiol 74:1620–1633

Kalinowski BE, Oskarsson A, Albinsson Y, Arlinger J, Ödegaard-Jensen A, Pedersen K (2004) Microbial leaching of trace elements from Randstad mine tailings. Geoderma 122:177–194

Kelly SD, Wu WM, Yang F, Criddle CS, Marsh TL, O'Loughlin EJ, Ravel B, Watson D, Jardine PM, Kemner KM (2010) Uranium transformations in static microcosms. Environ Sci Technol 44:236–242

Kimura T, Choppin GR (1994) Luminescence study on determination of the hydration number of Cm(III). J Alloys Compd 213–214:313–317

Krawczyk-Bärsch E, Lütke L, Moll H, Bok F, Steudner R, Rossberg A (2015) A spectroscopic study on U(VI) biomineralization in cultivated *Pseudomonas fluorescens* biofilms isolated from granitic aquifers. Environ Sci Pollut Res 22:4555–4565

Kuhner CH, Frank C, Grießhammer A, Schmittroth M, Acker G, Gößner A, Drake HL (1997) *Sporomusa silvacetica* sp. nov., an acetogenic bacterium isolated from aggregated forest soil. Int J Syst Bacteriol 47:352–358

Lloyd JR, Gadd GM (2011) The geomicrobiology of radionuclides. Geomicrobiol J 28:383–386

Lopez-Fernandez M, Fernandez-Sanfrancisco O, Moreno-Garcia A, Martin-Sanchez I, Sanchez-Castro I, Merroun ML (2014) Microbial communities in bentonite formations and their interactions with uranium. Appl Geochem 49:77–86

Lopez-Fernandez M, Cherkouk A, Vílchez-Vargas R, Sandoval R, Pieper D, Boon N, Sánchez-Castro I, Merroun ML (2015) Bacterial diversity in bentonites, engineered barrier for deep geological disposal of radioactive wastes. Microb Ecol. doi:10.1007/s00248-015-0630-7

Lovley DR, Philips EJP, Gorby YA, Landa ER (1991) Microbial reduction of uranium. Nature 350:413–416

Lütke L (2013) Interaction of selected actinides (U, Cm) with bacteria relevant to nuclear waste disposal. Doctoral thesis TU Dresden, Germany

Lütke L, Moll H, Bernhard G (2012) Insights on the Uranium(VI) speciation with *Pseudomonas fluorescen*s on a molecular level. Dalton Trans 41:13370–13378

Lütke L, Moll H, Bernhard G (2013) The U(VI) speciation influenced by a novel *Paenibacillus* isolate from Mont Terri Opalinus clay. Dalton Trans 42:6979–6988

Makarova KS, Aravind L, Wolf YI, Tatusov RL, Minton KW, Koonin EV, Daly MJ (2001) Genome of the extremely radiation-resistant bacterium *Deinococcus radiodurans* viewed from the perspective of comparative genomics. Microbiol Mol Biol Rev 65:44–79

Markai S, Andres Y, Montavon G, Grambow B (2003) Study of the interaction between europium (III) and *B*acillus subtilis: fixation sites, biosorption and reversibility. J Colloid Interface Sci 262:351–361

Mauclaire L, McKenzie J, Schwyn B, Bossart P (2007) Detection and identification of indigenous microorganisms in Mesozoic claystone core samples from the Opalinus clay formation (Mont Terri Rock Laboratory). Phys Chem Earth 32:232–240

Merroun ML, Selenska-Pobell S (2008) Bacterial interactions with uranium: an environmental perspective. J Contam Hydrol 102:285–295

Moll H, Merroun ML, Hennig C, Rossberg A, Selenska-Pobell S, Bernhard G (2006) The interaction of *Desulfovibrio äspöensis* DSM 10631^{T} with plutonium. Radiochim Acta 94:815–824

Moll H, Johnsson A, Schäfer M, Pedersen K, Budzikiewicz H, Bernhard G (2008a) Curium(III) complexation with pyoverdins secreted by a groundwater strain of *Pseudomonas fluorescens*. Biometals 21:219–228

Moll H, Glorius M, Bernhard G, Johnsson A, Pedersen K, Schäfer M, Budzikiewicz H (2008b) Characterization of pyoverdins secreted by a subsurface strain of *Pseudomonas fluorescens* and their interaction with uranium(VI). Geomicrobiol J 25:157–166

Moll H, Glorius M, Johnsson A, Schäfer M, Budzikiewicz H, Pedersen K, Bernhard G (2010) Neptunium(V) complexation by natural pyoverdins and related model compounds. Radiochim Acta 98:517–576

Moll H, Lütke L, Bachvarova V, Steudner R, Geißler A, Krawczyk-Bärsch E, Selenska-Pobell S, Bernhard G (2013a) Microbial diversity in Opalinus clay and interactions of dominant microbial strains with actinides. Wissenschaftlich-Technische Berichte, HZDR-036. Helmholtz-Zentrum Dresden-Rossendorf, Dresden

Moll H, Lütke L, Barkleit A, Bernhard G (2013b) Curium(III) speciation studies with cells of a groundwater strain of *Pseudomonas fluorescens*. Geomicrobiol J 30:337–346

Moll H, Lütke L, Bachvarova V, Cherkouk A, Selenska-Pobell S, Bernhard G (2014) Interactions of the Mont Terri Opalinus clay isolate *Sporomusa* sp. MT-2.99 with Curium(III) and Europium(III). Geomicrobiol J 31:682–696

Nyman JL, Marsh TL, Ginder-Vogel MA, Gentile M, Fendorf S, Criddle C (2006) Heterogeneous response to biostimulation for U(VI) reduction in replicated sediment microcosms. Biodegradation 17:303–316

Ohnuki T, Yoshida T, Ozaki T, Samadfam M, Kozai N, Yubuta K, Mitsugashira T, Kasama T, Francis AJ (2005) Interaction of uranium with bacteria and kaolinite clay. Chem Geol 220:237–243

Oren A (2002) Molecular ecology of extremely halophilic archaea and bacteria. FEMS Microbiol Ecol 39:1–7

Panak PJ, Nitsche H (2001) Interaction of aerobic soil bacteria with plutonium(VI). Radiochim Acta 89:499–504

Panak PJ, Raff J, Selenska-Pobell S, Geipel G, Bernhard G, Nitsche H (2000) Complex formation of U(VI) with *Bacillus*-isolates from a uranium mining waste pile. Radiochim Acta 88:71–76

Pantke C, Obst M, Benzerara K, Morin G, Ona-Nguema G, Dippon U, Kappler A (2012) Green rust formation during Fe(II) oxidation by the nitrate-reducing *Acidovorax* sp. strain BoFeN1. Environ Sci Technol 46:1439–1446

Pedersen K, Albinsson Y (1992) Possible effects of bacteria on trace-element migration in crystalline bed-rock. Radiochim Acta 58–59:365–369

Poulain S, Sergeant C, Simonoff M, Le Marrec C, Altmann S (2008) Microbial investigations in Opalinus clay, an argillaceous formation under evaluation as a potential host rock for a radioactive waste repository. Geomicrobiol J 25:240–249

Reitz T, Rossberg A, Barkleit A, Selenska-Pobell S, Merroun ML (2014) Decrease of U (VI) immobilization capability of the facultative anaerobic strain *Paenibacillus* sp. JG-TB8 under anoxic conditions due to strongly reduced phosphatase activity. PLoS One 9, e102447

Rodriguez-Diaz M, Lebbe L, Rodelas B, Heyrman J, De Vos P, Logan NA (2005) *Paenibacillus wynnii* sp. nov., a novel species harbouring the nifH gene, isolated from Alexander Island, Antarctica. Int J Syst Evol Microbiol 55:2093–2099

Rothstein A (1962) Functional implications of interactions of extracellular ions with ligands of the cell membrane. Circulation 26:1189–1200

Santelli CM, Orcutt BN, Banning E, Bach W, Moyer CL, Sogin ML, Staudigel H, Edwards KJ (2008) Abundance and diversity of microbial life in ocean crust. Nature 453:653–656

Selenska-Pobell S, Kampf G, Flemming K, Radeva G, Satchanska G (2001) Bacterial diversity in soil samples from two uranium waste piles as determined by rep-APD, RISA and 16S rDNA retrieval. Antonie Van Leeuwenhoek 79:149–161

Shapiro J (1967) Induced rapid release and uptake of phosphate by microorganism. Science 155:1269–1271

Sharp JO, Lezama-Pacheco JS, Schofield EJ, Junier P, Ulrich KU, Chinni S, Veeramani H, Margot-Roquier C, Webb SM, Tebo BM, Giammar DE, Bargar JR, Bernier-Latmani R (2011) Uranium speciation and stability after reductive immobilization in aquifer sediments. Geochim Cosmochim Acta 75:6497–6510

Stewart EJ (2012) Growing unculturable bacteria. J Bacteriol 194:4151–4160

Stroes-Gascoyne S, Schippers A, Schwyn B, Poulain S, Sergeant C, Simonoff M, Le Marrec C, Altmann S, Nagaoka T, Mauclaire L, McKenzie J, Daumas S, Vinsot A, Beaucaire C, Matray JM (2007) Microbial community analysis of Opalinus clay drill core samples from the Mont Terri underground research laboratory, Switzerland. Geomicrobiol J 24:1–17

Suzuki Y, Banfield JF (2004) Resistance to, and accumulation of, uranium by bacteria from a uranium-contaminated site. Geomicrobiol J 21:113–121

Takai K, Nakamura K, Toki T, Tsunogai U, Miyazaki M, Miyazaki J, Hirayama H, Nakagawa S, Nunoura T, Horikoshi K (2008) Cell proliferation at 122°C and isotopically heavy CH_4 production by a hyperthermophilic methanogen under high-pressure cultivation. Proc Natl Acad Sci USA 105:10949–10954

Texier AC, Andres Y, Illemassene M, Le Cloirec P (2000) Characterization of lanthanide ions binding sites in the cell wall of *Pseudomonas aeruginosa*. Environ Sci Technol 34:610–615

Thury M, Bossart P (1999) The Mont Terri Rock laboratory, a new international research project in a Mesozoic shale formation, in Switzerland. Eng Geol 52:347–359

Urios L, Marsal F, Pellegrini D, Magot M (2012) Microbial diversity of the 180 million-year-old Toarcian argillite from Tournemire, France. Appl Geochem 27:1442–1450

Urios L, Marsal F, Pellegrini D, Magot M (2013) Microbial diversity at iron-clay interfaces after 10 years of interaction inside a deep argillite geological formation (Tournemire, France). Geomicrobiol J 30:442–453

Voet D, Voet JG, Pratt CW (2002) Lehrbuch der Biochemie. Wiley, Germany

Wouters K, Moors H, Boven P, Leys N (2013) Evidence and characteristics of a diverse and metabolically active microbial community in deep subsurface clay borehole water. FEMS Microbiol Ecol 86:458–473

Yee N, Benning LG, Phoenix VR, Ferris FG (2004) Characterization of metal-cyanobacteria sorption reactions: a combined macroscopic and infrared spectroscopic investigation. Environ Sci Technol 38:775–782

Yutin N, Galperin MY (2013) A genomic update on clostridial phylogeny: Gram-negative spore formers and other misplaced clostridia. Environ Microbiol 15:2631–2641

Zhengji Y (2010) Microbial removal of uranyl by uranyl reducing bacteria in the presence of Fe (III) (hydr)oxides. J Environ Radioact 101:700–705